

K^+ Three-Body Leptonic Decay Modes*

FRED R. EISLER, SUN Y. FUNG,† SAMUEL L. MARATECK,‡
STUART L. MEYER,§ AND RICHARD J. PLANO

Rutgers, The State University, New Brunswick, New Jersey

(Received 18 December 1967)

The $K_{\mu 3}^+ \rightarrow \pi^0 + \mu^+ + \nu$ and $K_{e 3}^+ \rightarrow \pi^0 + e^+ + \nu$ decay-mode Dalitz-plot distributions were studied for lepton momenta below 120 MeV/c, using an exposure of the Brookhaven 30-in. propane bubble chamber to a stopping beam of K^+ mesons. The vector momentum of the π^0 was obtained with a typical error of 5% by considering only those events in which both γ rays from the π^0 decay converted to electron-positron pairs. Both decay modes are consistent with a pure vector interaction. 78 $K_{\mu 3}$ events yield the results, assuming ξ to be independent of momentum transfer: $\text{Re}\xi = -0.5 \pm 0.9$, $|\text{Im}\xi| = 0.0_{-0.0}^{+2.3}$, and a discrimination of 150:1 against a second value of $\text{Re}\xi = -5.3 \pm 0.7$. There were 90 $K_{e 3}$ events consistent with a constant form factor f^+ , giving $\lambda_+ = -0.02_{-0.12}^{+0.08}$.

I. INTRODUCTION

THE three-body leptonic decay modes of the K^+ ,

$$\begin{aligned} K_{\mu 3}^+ &\rightarrow \pi^0 + \mu^+ + \nu, \\ K_{e 3}^+ &\rightarrow \pi^0 + e^+ + \nu, \end{aligned} \quad (1)$$

have been studied extensively¹ in an attempt to gain further insight into the structure of the weak interaction. Assuming the $K_{l 3}$ decays to proceed by a pure vector interaction, as is consistent with previous experiments,^{2,3} the matrix element for $K_{l 3}$ decay may be written as⁴

$$M = \langle \pi | J_\alpha | K \rangle \langle \nu | j_\alpha | l \rangle. \quad (2)$$

We use the notation of Ref. 3 with $j_\alpha = \gamma_\alpha(1 + \gamma_5)$, $J_\alpha = f^+(q^2)(q_K + q_\pi)_\alpha + f^-(q^2)(q_K - q_\pi)_\alpha$, where q_π and q_K are the π and K four-momenta and $q^2 = (q_K - q_\pi)^2$ is the four-momentum transfer between the π and the K . The Dalitz-plot distribution is a function only of

$\xi = f^-/f^+$ for the $K_{\mu 3}$ decay mode, assuming constant form factors, and of f^- for the $K_{e 3}$ decay mode since the term proportional to f^- in $K_{e 3}$ decay is proportional to m_e^2 and cannot be discerned with currently available statistics. It is customary to express the momentum transfer dependence of the form factors by a first-order expansion:

$$f^\pm(q^2) = f^\pm(0)(1 + \lambda_\pm q^2/m_\pi^2). \quad (3)$$

We have measured the real and imaginary parts of ξ for $K_{\mu 3}$ decay and f^- for $K_{e 3}$ decay and have also verified that both decay modes are consistent with a pure vector interaction.

In Sec. II, the procedures used to obtain the photographs and to extract a set of events suitable for direct comparison with the theory are described. The technique and accuracy with which π^0 decays were reconstructed were checked, using the monoenergetic π^0 from $K_{\pi 2}$ decay at rest as described in Sec. III. Possible sources of background are discussed in Sec. IV showing that in the region of the Dalitz plot for which the lepton momentum is less than 120 MeV/c—the region used in the analysis—the backgrounds are negligible relative to the statistical accuracy of the experiment. In particular, since the $\tau'(K^+ \rightarrow \pi^+ + \pi^0 + \pi^0)$ decay mode is strongly discriminated against, the $K_{\mu 3}$ decay can be investigated down to the lowest muon momenta—a region particularly sensitive to ξ . Finally, a detailed comparison with theory is described in Sec. V.

II. EXPERIMENTAL PROCEDURE

Approximately 150 000 pictures containing 10^6 K^+ decays were taken in the BNL 30-in. propane chamber placed in the stopping K^+ beam of the alternating gradient synchrotron at Brookhaven National Laboratory. A typical picture contained about 7 stopping K^+ mesons and 20 pions. The pions cluttered the pictures but otherwise caused no trouble as they generally passed through the picture without interacting or stopping. Propane, which has a density of 0.41 g/cm³ and a radiation length of 109 cm, was chosen for the sensitive liquid to provide a reasonable probability of converting a γ ray to an electron-positron pair (about 20%) while

* Work supported in part by the National Science Foundation.

† Present address: Physics Department, University of California, Riverside, Calif.

‡ Submitted in partial fulfillment of the Ph.D. degree at Rutgers, the State University, New Brunswick, N. J. Present address: Physics Department, University of Pennsylvania, Philadelphia, Pa.

§ Present address: Physics Department, Northwestern University, Evanston, Ill.

¹ N. Cabibbo, in *Proceedings of the Thirteenth International Conference on High-Energy Physics, Berkeley, 1966* (University of California Press, Berkeley, 1967), p. 29.

² V. Bisi, G. Borreani, R. Cester, A. de Benedetti, M. I. Ferrero, C. M. Garelli, A. Martzri-Chisea, B. Quassati, G. Rinaudo, M. Bigone, and A. E. Werbrouck, *Phys. Rev.* **139**, B1068 (1965); J. L. Brown, J. A. Kadyk, G. H. Trilling, R. T. Van de Walle, B. P. Roe, and D. Sinclair, *Phys. Rev. Letters* **8**, 450 (1962); D. Cutts, T. Elioff, and R. Stiening, *Phys. Rev.* **138**, B969 (1965); V. A. Smirnitski and A. O. Weissenberg, *Phys. Rev. Letters* **12**, 223 (1964); G. Borreani, G. Gidal, G. Rinaudo, A. Werbrouck, A. Daforio, C. Garelli, S. Natali, and M. Vallani, *Phys. Rev.* **140**, B1686 (1965); U. Camerini, R. D. Hantman, R. March, D. Murphree, G. Gidal, G. Kalmus, W. Powell, R. Pu, C. Sandler, S. Natali, and M. Vallani, *Phys. Rev. Letters* **14**, 989 (1965); G. Gidal, W. Powell, R. March, and S. Natali, *ibid.* **13**, 95 (1964); E. Bellotti, E. Fiormi, and A. Pullia, *Phys. Letters* **20**, 690 (1966).

³ A. Callahan, N. Camerini, R. Hantman, R. March, P. Murphree, G. Gidal, G. Kalmus, W. Powell, C. Sandler, R. Pu, S. Natali, and M. Vallani, *Phys. Rev.* **150**, 1153 (1966).

⁴ S. W. MacDowell, *Nuovo Cimento* **6**, 3305 (1957); N. Brene, L. Egardt, and B. Quist, *Nucl. Phys.* **22**, 553 (1961).

still allowing reasonably precise momentum measurements from curvature (typically 15% for a fast pion).

Events in which two γ rays pointed back to a common K^+ vertex in all three views were scanned for and 3500 were found. An attempt was immediately made to identify the K^+ secondary using the following criteria: If the K^+ secondary decayed into a clear electron, it was identified as a muon. If it decayed into a clear muon, it was identified as a pion. If it did not decay, but was minimum-ionizing and rotated through more than 90° or produced a δ ray of momentum greater than 5 MeV/c, it was identified as an electron. Finally, if it scattered and produced a recoil proton, or scattered through more than 45° , it was identified as a pion. The two γ -ray events were then measured, using three points per track in three views on film-plane digitizers. The measurement accuracy in the plane parallel to the camera plane was 0.015 cm in the chamber.

The programs used to analyze the events included the geometrical reconstruction program NP54⁵ and the kinematical fitting program GRIND.⁶ The kinematic fitting was done as follows: The two γ rays were first fitted using the direction from the K^+ vertex to the electron pair vertex and the vector momenta of the electrons. The γ rays were then fitted to a π^0 (1C) where 1C signifies that the fit has one degree of freedom and is called constraint class 1. Finally, the event was fitted to the K_{π^2} ($K^+ \rightarrow \pi^+\pi^0$) (4C), K_{e3} (1C), and $K_{\mu 3}$ (1C) and τ' (1C) modes. In all cases, the event was fitted assuming both that the K^+ was at rest and that it decayed in flight.

A fit was accepted only if the χ^2 probability for the π^0 fit was greater than 5% and the χ^2 probability for the three-body fits was greater than 5%. The χ^2 probability distribution for π^0 fits, although flat above the 5% level, began to rise below it and rose sharply below the 2% level. An investigation showed that this anomaly was due to the fact that for fits below 5% probability, the γ rays did not always originate from the K^+ vertex in the event being analyzed. The χ^2 probability distribution for the three-body modes was also flat above the 5% level. Since the χ^2 for an event depended only weakly on the π^0 and lepton energies, these cutoffs did not significantly affect the final Dalitz-plot distribution.

After the fitting was done, physicists carefully examined the events on the scanning table and rejected all those in which the K^+ ionization was not consistent with a decay at rest and those in which the two γ rays did not point back to the K^+ vertex in all three views. They then attempted to classify the events as $K_{\mu 3}$, K_{e3} , or K_{π^2} decays by examining the mass-dependent characteristics of the K^+ secondary. The classification of the $K_{\mu 3}$ and K_{e3} events was done for those events in

which the K^+ secondary, when corrected for energy loss as a muon, had a momentum lower than 140 MeV/c.

A. $K_{\mu 3}$

To be classified as a $K_{\mu 3}$ decay, the K^+ secondary had to stop in the chamber and decay into a positron. The muon momentum was measured from range. The geometrical detection efficiency for such configurations dropped considerably above $P_\mu = 120$ MeV/c; consequently this momentum was chosen as the upper momentum cutoff for the $K_{\mu 3}$ events.

Physicists then examined the 173 events identified as $K_{\mu 3}$ decays which had acceptable π^0 decay fits, and eliminated from the sample: (1) the 34 events in which the K^+ secondary kinked in a fashion consistent with a $\pi\text{-}\mu\text{-}e$ decay chain or in which the γ 's did not point back, (2) the 10 events which were consistent with being a $K_{\mu 3}$ decay in flight and not with a $K_{\mu 3}$ decay at rest, (3) the 21 events which fit τ' at-rest or in-flight decays, and (4) the 15 events which had P_μ greater than 120 MeV/c. This reduced the sample to 93 events. Of this sample, 78 fit the $K_{\mu 3}$ at-rest hypothesis. The remaining 15 events are consistent with the number that the backgrounds (discussed in Sec. IV) should contribute to the sample and with the number of real $K_{\mu 3}$ events that should fit with a probability of less than 5%. Because of the difficulty in finding muons with P_μ less than 25 MeV/c ($T_\mu = 3$ MeV), this was used as the lower muon momentum limit.

B. K_{e3}

The K_{e3} candidates were obtained from the sample of events in which the K^+ secondary was identified as an electron (see beginning of Sec. II). The positron momentum was obtained from curvature. In order to facilitate the identifications, only events in which the absolute value of the K^+ secondary dip was less than 70° were used.

Physicists examined the photographs of the 309 events, in which the γ 's fit a π^0 with probability greater than 5% and where the K^+ secondary dip was less than 70° from the original sample of 566 events in which the K^+ secondary was not identified as a pion or muon and which had P_μ less than 140 MeV/c. They then attempted to separate the electrons from the muons and pions for every event in this sample by (1) checking the scanner's identification of the electrons and reapplying the same identification criteria used by them to the unidentified events; (2) classifying a K^+ secondary as an electron if its ionization was inconsistent with that expected of a muon (pion).

By eliminating obvious errors and those events which fit K^+ decays in flight, the sample was reduced to 206 events. $P_e = 120$ MeV/c was chosen as the upper momentum limit for K_{e3} events since only for P_e less than 120 MeV/c was it always possible to uniquely identify the secondary as an electron on the one hand or

⁵ R. J. Plano and D. H. Tycko, Nucl. Instr. Methods **20**, 458 (1963).

⁶ GRIND 709 Kinematics Program Manual, CERN, Geneva, 1963 (unpublished).

as a pion or muon on the other. Specifically, below 120 MeV/c there were 104 e^+ , 26 $\mu^+(\pi^+)$, and 16 π^+ scatters; above 120 MeV/c there were 30 e^+ , 10 $\pi^+(\mu^+)$, 6 π^+ scatters, and 14 events in which the secondary could have been either a e^+ or μ^+ . Of the 104 identified electrons, 90 fit the K_{e3} at-rest hypothesis with χ^2 probabilities greater than 5%. The 14 events which did not fit are consistent with the sum of the 5 events expected to fit with probability less than 5% plus the 7 events expected from the background due to unassociated γ rays. This background will be discussed in Sec. IV.

Since the scanners looked for converted γ rays first and then the K^+ vertex, and because the over-all appearance of the electron-positron pairs depends only weakly on the π^0 energy, the identification of an event is reasonably independent of where it falls on the Dalitz plot. A second scan verified this. The geometrical detection efficiency was calculated as a function of P_{π^0} and P_{μ} , using Monte Carlo techniques, and was found to be essentially independent of P_{π^0} .

Since the decay positron in K_{e3} decays can be identified with 100% confidence below $P_e = 120$ MeV/c, and because the π^0 detection efficiency is independent of T_{π^0} , the K_{e3} detection efficiency is constant over the utilized region of the Dalitz plot.

III. $K_{\pi 2}$ DECAY

The fact that the $K_{\pi 2}$ decay mode at rest yields a monochromatic π^0 momentum spectrum at 205 MeV/c provides a check on the precision with which the π^0 momentum can be reconstructed in this experiment. From a sample of 253 events in which the charged secondary had been identified as a π^+ by the scanners (see Sec. II), 152 events fit a π^0 decay with a probability greater than 5%. Physicists examined these 152 events on the scanning table and eliminated obvious errors, including τ events, from the sample, thereby reducing it to 108 events. On the basis of $K_{\pi 2}$ kinematics and K^+ ionization, 12 events which were consistent with being in-flight $K_{\pi 2}$ decays were rejected. The kinematics for

7 of the remaining 96 events were inconsistent with the kinematics for $K_{\pi 2}$ decays at rest. These events will be used to estimate the background to K_{e3} events (discussed in Sec. IV) due to electron-positron pairs which appear to point back to the same K^+ vertex and which fit a π^0 with a probability greater than 5% but which actually come from two different sources. In Fig. 1 the π^0 momentum plot for all 96 events is shown. The background events are shown in black. The plot of the 89 real events peaks at the expected momentum of 205 MeV/c and has a half-width of 10 MeV/c. The $\pi^+-\pi^0$ opening angle distribution peaks at 177° with a half-width of 3° and is thus consistent with the $\pi^+-\pi^0$ opening angle being, as it should, 180° .

IV. BACKGROUNDS

A. Background in K_{e3} Decays

(a) If the muon has so little energy ($T_{\mu} < 3$ MeV) that it cannot be detected, the $\mu-e$ sequence looks like an electron. However, less than $\frac{1}{2}$ $K_{\mu 3}$ with $T_{\mu} < 3$ MeV is expected from phase-space considerations and even less than that is expected to both look like and fit a K_{e3} .

(b) Events in which two γ rays point back to the same K^+ vertex and also fit the π^0 decay hypothesis but in which one or both of the two γ rays originate at another K^+ vertex constituted a possibly serious background. In order to determine the extent of this background, events were constructed from unrelated γ rays having the same momentum and angular spectrum as the γ rays measured in the experiment.

To do this the measurements with errors of a γ ray were replaced by those of a γ ray from another event. If the χ^2 probability for a π^0 decay into these two unrelated γ rays was greater than 5%—which happened $\frac{1}{3}$ of the time—then the π^0 and the charged secondary in the original event were fitted to a K_{e3} decay at rest. It was found that $\frac{1}{3}$ of the random γ events constructed in this way fit a K_{e3} decay at rest with a probability greater than 5%. The probability for a random γ ray to appear to be associated with a K^+ vertex can be determined, using $K_{\pi 2}$ decays which are highly constrained (4C). From this an upper limit can be placed on the random π^0 background, since it is highly unlikely that the K^+ , π^+ secondary and random π^0 will fit either a $K_{\pi 2}$ at rest or in flight. In the study of the $K_{\pi 2}$ made in Sec. III it was seen that the ratio of fake π^0 decays to real ones was 1/13. Since the γ -ray momentum spectra from all sources are similar, the ratio 1/13 also represents the ratio of fake π^0 decays to real ones in the K_{e3} mode. Thus of our 104 K_{e3} candidates for which the two γ rays fit a π^0 and the electron has a momentum below 120 MeV/c, $1/13 \times 104 = 8$ have a fake π^0 ; and of these, $\frac{1}{3} \times 8 = 1.6$ would be expected to fit K_{e3} decay. This background of less than two events is negligible considering our statistics.

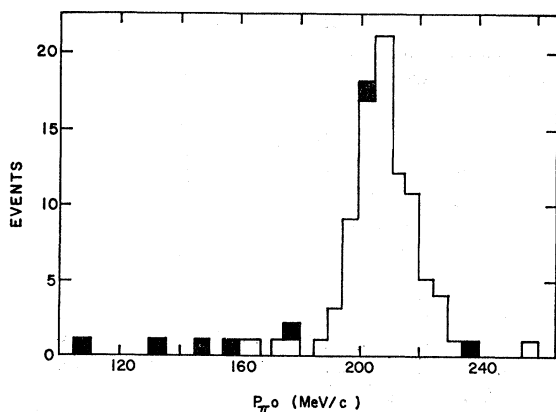


FIG. 1. π^0 momentum spectrum for 96 identified pion events. Background events are shown in black.

B. Background in $K_{\mu 3}$ Decays

(a) First the background from τ' decays is discussed. A τ' can simulate a $K_{\mu 3}$ when the π - μ decay angle is so small that the scanners identify the π and its decay μ as a muon, a problem aggravated by the multiple scattering of the stopping π and μ and the short range of the μ (3 mm).

Figure 2, which exhibits the kinematics of τ' and $K_{\mu 3}$ decays at rest, is very useful in estimating this background. It is clear from this figure that τ' decays at rest in which both γ rays come from the same π^0 cannot fit a $K_{\mu 3}$ at rest. A background from τ' decays does arise, however, from (1) τ' events in which both of the γ rays do not come from the same π^0 ; (2) τ' decays in flight in which the K^+ because of its heavy ionization ($P_K < 200$ MeV/c) is indistinguishable from a K^+ at rest.

To estimate the extent of this background, all 700 two- γ events in which the K^+ secondary stopped and clearly decayed into a muon were fitted to a τ' decay at rest. The events in which the γ rays fit a π^0 but in which the resulting π^0 and the π^+ did not fit a τ' at rest were fitted to $K_{\mu 3}$ at rest. Physicists investigated the K^+ ionization and rejected any K^+ which was inconsistent with decaying at rest leaving 12 events which fit $K_{\mu 3}$ at rest. To determine the fraction of these 12 events which would also have an invisible π - μ sequence, the K^+ decay in which each K^+ positive-charged secondary is known to be a π^+ , namely,

$$K^+ \rightarrow \pi^+ + \pi^+ + \pi^-,$$

was investigated. It was found that in from 5 to 10% of the cases, depending on the region of the film investigated, the decay μ^+ at the end of the π^+ could not be detected. Using the 10% figure as the fraction of undetectable π^+ decays, it is seen that the 12 events which fit $K_{\mu 3}$ and which have clearly identifiable pions as secondaries represent 90% of the τ' decays which fit $K_{\mu 3}$; consequently there are 1.3 events which fit and look like the $K_{\mu 3}$ mode, but are in fact τ' decays. This is an upper limit since the 10% figure and not the 5% one was used for the fraction of undetectable π^+ decays.

(b) We now discuss the background from $K_{\pi 2}$ events

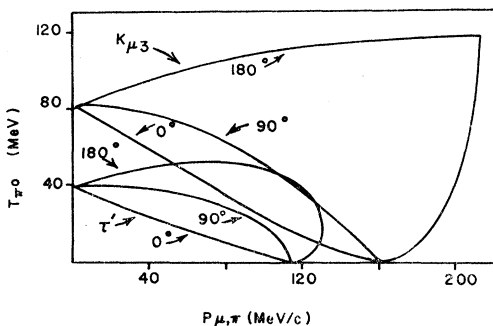


FIG. 2. Kinematics for τ' and $K_{\mu 3}$ decays at rest. The curves are contours of constant π^0 - μ^+ or π^0 - π^+ opening angles.

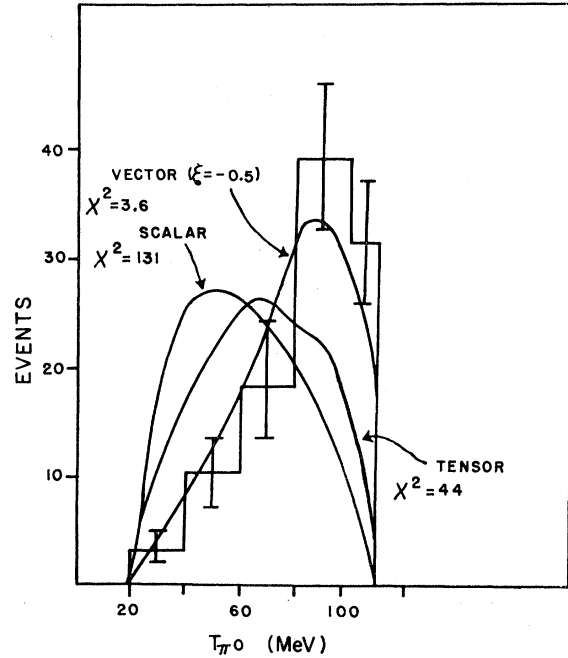


FIG. 3. Normalized $K_{\mu 3}$ theoretical T_{π^0} spectra ($3 < T_{\mu} < 55$ MeV) and experimental spectrum for 78 $K_{\mu 3}$ events. The χ^2 for each fit is shown.

in which the opening angle $\Theta_{\pi\mu}$ between the π^+ and the μ^+ , is small, and thus the π - μ sequence looks like a μ^+ . The total range of the π and μ can be equivalent to a muon momentum below 120 MeV/c only if the π decays at a momentum above 195 MeV/c. Including the solid angle factor, less than one pion in our sample is expected to simulate an acceptable $K_{\mu 3}$.

(c) The background to $K_{\mu 3}$ decays from random- γ 's corresponding to the one investigated in the section on K_{e3} backgrounds is negligible since the muon momentum is known at least 20 times more accurately than the electron momentum, and thus it is much more difficult for a stopping muon and a fake π^0 to fit a $K_{\mu 3}$ decay at rest.

V. ANALYSIS OF DATA

A. $K_{\mu 3}$ Analysis

In order to show that our events are consistent with a pure vector interaction, the Dalitz-plot density was integrated with respect to P_{μ} from 25 to 120 MeV/c for the scalar, vector, and tensor interactions. Figure 3 shows the normalized theoretical spectra and the experimental T_{π^0} spectrum corrected for the geometrical detection efficiency. The χ^2 fit to the vector curve for $\text{Re}\xi = -0.5$ gives a probability of 44%, whereas the χ^2 fit to the scalar and tensor curves both give a probability less than 1%. In the ensuing analysis it will be assumed that the interaction is vector.

$\text{Re}\xi$, assuming $|\text{Im}\xi| = 0$, was determined by three different although not independent fits to the data (1)

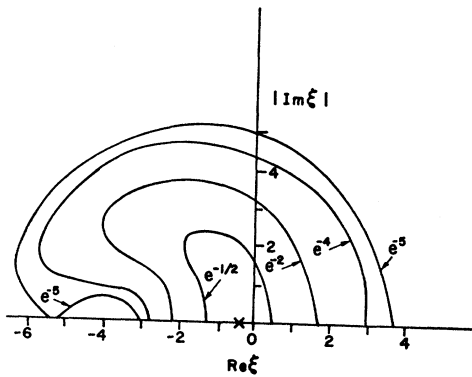


FIG. 4. Maximum-likelihood fit to partitioned Dalitz plot for $\text{Re}\xi$ versus $|\text{Im}\xi|$. The curves are contours of constant likelihood normalized to unity at the peak ($\text{Re}\xi = -0.5 \pm 0.9$; $|\text{Im}\xi| = 0.05_{0.0}^{+2.3}$), shown as an X.

by fitting to the over-all Dalitz plot, (2) by fitting to the Dalitz plot subdivided into independent bins in P_μ^3 (this fit is thus independent of the muon scanning efficiency but uses the π^0 - μ angular correlation as a function of P_μ), and (3) by fitting to the π^0 energy spectrum. This procedure permits a choice between the reduction in systematic uncertainties versus the increase in statistical error as information is discarded.

The maximum likelihood fitted to the Dalitz-plot density yielded two peaks in the likelihood plot, one at $\text{Re}\xi = -0.5 \pm 0.9$ and a secondary peak at $\text{Re}\xi = -4.7_{-0.7}^{+0.6}$.

The ratio of the likelihoods was

$$\frac{L(\text{Re}\xi = -0.5)}{L(\text{Re}\xi = -4.7)} = 800:1.$$

The Dalitz plot was then divided into bins (5 MeV in T_μ) parallel to the π^0 energy axis and the likelihood function for a given bin was normalized to the number of events in that bin. The advantage of normalizing the events in this way is that the resultant likelihood function is independent of any possible μ^+ energy bias while providing almost equivalent information on $\text{Re}\xi$.

The likelihood function peaks at $\text{Re}\xi = -0.5 \pm 0.9$ and $\text{Re}\xi = -5.3 \pm 0.7$, but now the likelihood ratio is

$$\frac{L(\text{Re}\xi = -0.5)}{L(\text{Re}\xi = -5.3)} = 150:1.$$

This ratio of 150:1 corresponds to a 2.7 standard-deviation discrimination against the larger negative peak as compared to 3.2 standard deviations when the likelihood ratio is 800:1. Since the statistics on the muon energy scanning bias are poor, the discrimination of 150:1 is systematically superior.

Finally, a maximum-likelihood fit was applied to the π^0 energy spectrum only, with the following result:

$$\text{Re}\xi = -1.04_{-1.7}^{+1.2}.$$

The error is now 50% larger and the two peaks are barely resolvable. Thus by fitting to the T_{π^0} spectrum only, one loses important information.

In summary, by eliminating the muon energy spectrum information from the Dalitz-plot analysis, any possible muon energy bias has also been eliminated but no significant information is lost. It was therefore decided to use this technique for the remaining analysis.

Next, a two-dimensional maximum-likelihood fit in which both $\text{Re}\xi$ and $|\text{Im}\xi|$ were varied was applied to the Dalitz-plot density ρ . Since ρ depends on $\text{Im}\xi$ only

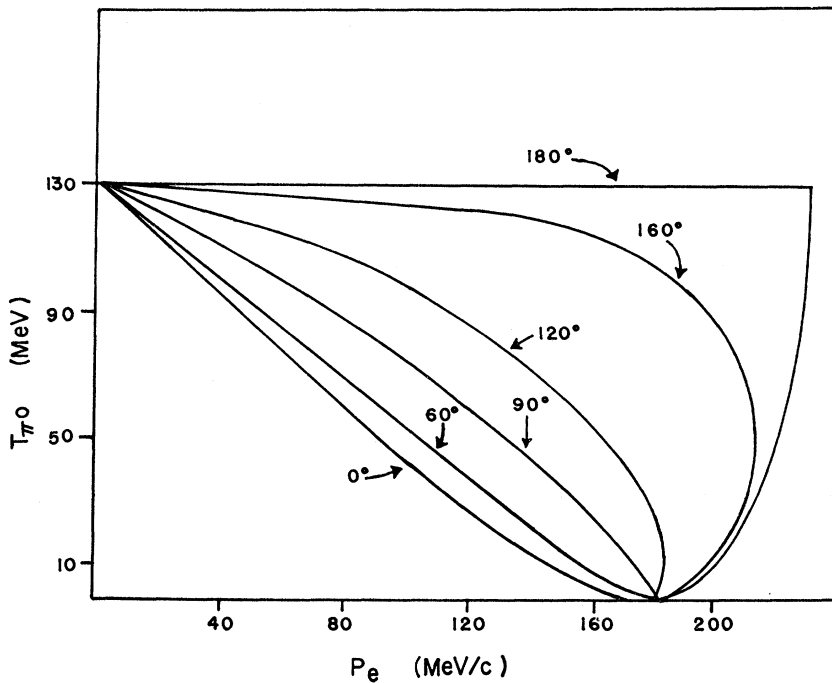


FIG. 5. Kinematics for K_{e3} decays at rest. Curves are contours of constant π - e opening angles.

through the $|\xi|^2$ term, the analysis of ρ can only yield information on $|\text{Im}\xi|$. In Fig. 4 are plotted the contours of constant likelihood normalized to the most likely value of ξ which is shown as an \times on the plot. By reading the numbers at the $e^{-1/2}$ contour, one obtains $\text{Re}\xi = -0.5 \pm 0.9$ and $|\text{Im}\xi| = 0.0_{-0.0}^{+2.3}$. The value of $\text{Re}\xi$ obtained is practically independent of $|\text{Im}\xi|$ since the $e^{-1/2}$ contour is almost parallel to the $|\text{Im}\xi|$ axis, unlike similar fits³ which exclude the low P_μ portion of the Dalitz plot.

B. K_{e3} Analysis

One sees from the K_{e3} kinematics shown in Fig. 5 that for the region of the Dalitz plot corresponding to P_e below 120 MeV/c and $\Theta_{\pi^0 e}$ near 180° the contours of constant opening angles are almost parallel to lines of constant T_{π^0} . Consequently, the fitting procedure does not improve the precision to which P_e is known in this region. This means that in this or any experiment in which the decay positron momentum error is large, an analysis of the K_{e3} Dalitz-plot density does not yield much more accurate information than a corresponding analysis of the π^0 kinetic-energy spectrum, and may be subject to greater systematic biases.

In order to determine the nature of the interaction, the T_{π^0} data were fitted to the theoretical T_{π^0} spectra for the vector, scalar, and tensor interactions obtained by integrating the theoretical Dalitz-plot densities from $T_e = 0$ to $T_e = 120$ MeV. No form-factor dependence on q^2 was assumed. In Fig. 6 the experimental as well as the normalized theoretical T_{π^0} spectra are shown. The χ^2 probability for the vector fit is 95%, whereas the χ^2 probability for the tensor and scalar fits are each less than 1%.

A fit of the experimental distribution in the opening angle $\alpha_{\pi\nu}$ between the π^0 and the neutrino in the dilepton center-of-mass system to the theoretically expected spectra for the scalar, vector, and tensor distributions yielded a χ^2 probability for the vector fit of 45%, and a χ^2 probability for tensor and scalar fits of less than 1%. Since we cut off at $T_e = 120$ MeV, $\cos\alpha_{\pi\nu}$ and q^2 are no longer independent variables; consequently the $\cos\alpha_{\pi\nu}$ spectrum is not independent of the form-factor dependence on q^2 .

The f^+ dependence on q^2 was explored by performing a maximum-likelihood fit to λ_+ using first the Dalitz-plot density and then only the T_{π^0} spectrum.

The Dalitz-plot fit yields

$$\lambda_+ = -0.01_{-0.12}^{+0.08}.$$

The fit to the π^0 kinetic-energy spectrum only, which we feel is systematically superior because of the difficulties in measuring the decay positron energy, yields $\lambda_+ = -0.02_{-0.12}^{+0.08}$.

VI. CONCLUSIONS

Our results are consistent with a pure vector interaction in both K_{e3} and $K_{\mu 3}$ decay and are thus com-

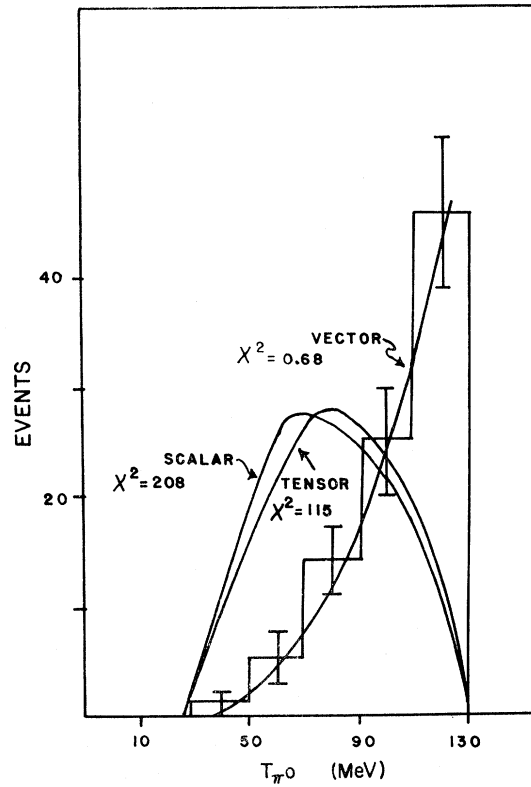


FIG. 6. Normalized K_{e3} theoretical T_{π^0} spectra ($T_e = 120$ MeV) and experimental K_{e3} spectrum for 90 K_{e3} events. The χ^2 for each fit is shown.

patible with the universal $V-A$ theory. The form factor in K_{e3} is consistent with no energy dependence ($\lambda_+ = -0.02_{-0.12}^{+0.08}$). We are unable to determine the energy dependence of the form factor in $K_{\mu 3}$ decay due to the restricted region of the Dalitz plot examined, but this region is quite sensitive to ξ , yielding $\text{Re}\xi = -0.5 \pm 0.9$ and $|\text{Im}\xi| = 0.0_{-0.0}^{+2.3}$. Time-reversal invariance predicts $|\text{Im}\xi|$ to be zero, but our error could well be too large to detect a possible effect.¹ The value of $\text{Re}\xi$ is consistent with several models^{7,8} but is not precise enough to provide a decisive check.

ACKNOWLEDGMENTS

We thank Dr. A. Prodell and the staffs of the BNL 30-in. propane chamber and the AGS for their indispensable assistance in obtaining the pictures used in the analysis. We thank also the members of the measuring and scanning staff at Rutgers University for their fine work, in particular, Harold Katz and Bu Kim. It is a pleasure to acknowledge the contributions of John Pasco, Richard Nieperont, Ken Werner, and Hilton Zepp in computing and bookkeeping.

⁷ P. Dennery and H. Primakoff, Phys. Rev. **131**, 1334 (1963).

⁸ T. Das, Phys. Rev. Letters **17**, 671 (1966).